



# Study on the basic centers and active oxygen species of solid-base catalysts for oxidation of iso-mercaptans

Yufen Zhang<sup>a,b,\*</sup>, Zhenyi Liu<sup>b</sup>, Shenyong Ren<sup>a</sup>, Wennian Wang<sup>a</sup>, Baojian Shen<sup>a</sup>

<sup>a</sup> State Key Laboratory of Heavy Oil Processing and College of Chemical Engineering, China University of Petroleum, Beijing 102249, PR China

<sup>b</sup> Beijing SJ Environmental Protection and New Material Co. Ltd, Beijing 100080, PR China



## ARTICLE INFO

### Article history:

Received 3 September 2013

Received in revised form

19 December 2013

Accepted 8 January 2014

Available online 15 January 2014

### Keywords:

Basic centers

Active oxygen species

Iso-mercaptop

Sweetening

Hydrogenated gasoline

## ABSTRACT

It is a challenge to remove mercaptans as well as to keep octane value in clean gasoline production. In this work, gas–liquid–solid heterogeneous base-catalyzed oxidation of *tert*-butyl thiol by molecular oxygen was investigated. The reactivity and stability of modified MgO catalysts were studied. The catalysts were further characterized by XRD, FT-IR, CO<sub>2</sub>-TPD, H<sub>2</sub>-TPD, O<sub>2</sub>-TPD and EPR. Compared with commercial cobalt phthalocyanine catalyst (CoPc catalyst), the modified MgO catalyst displayed an enhanced stability to the oxidation of *tert*-butyl thiol, and the catalytic lifetime is 10 h longer than that of CoPc catalyst at 3.0 h<sup>-1</sup> of LHSV. It was found that the active sites of the catalysts are defects and basic centers. In addition, the basic sites responsible for the reactivity are mainly the medium and strong basic centers. It is interesting that the part of O<sub>3C</sub><sup>2-</sup>–Mg<sub>3C</sub><sup>2+</sup> provides medium basic centers, however, the other part of it supplies as strong basic centers. It was demonstrated that superoxide anions O<sub>2</sub><sup>-</sup> served as the active oxygen species.

© 2014 Elsevier B.V. All rights reserved.

## 1. Introduction

Hydro-desulfurization (HDS) of fluid catalytic cracking (FCC) gasoline is a promising process from the environmental point of view [1–5]. Octane-boosting olefins in FCC gasoline are often saturated during the process of hydro-treatment, which was performed under the conditions of high pressure and high temperature, leading to the loss of the octane value of the gasoline [6]. Therefore, it is challenging to keep a high octane value during the HDS of FCC gasoline under these harsh conditions. One of the solutions is deep HDS should be performed under mild conditions. However, it was also reported that under mild conditions of HDS, olefins could form thiols through recombination with H<sub>2</sub>S produced during HDS. Unfortunately, these new mercaptans were mostly iso-mercaptans and macromolecular thiols [1,7–10].

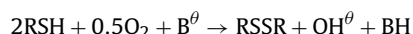
Mercaptans are adverse to environment because of the foul odors and the SO<sub>x</sub> it produce. Moreover, the acidity of mercaptans is corrosive to metals, which is harmful to storage and application of hydrocarbons it contain. Therefore, mercaptans removal is necessary to clean fuel production. Generally, extracting or converting are two ways used in mercaptans removal technology, and such

processes are usually called sweetening in the petroleum industry [11,12].

Cobalt phthalocyanine (CoPc) catalyst system was successful to catalyze the oxidation reaction of mercaptans to disulfides under caustic conditions in the presence of molecular oxygen [13–17]. But iso-mercaptans and macromolecular thiols cannot be easily oxidized through conventional sweetening process by using CoPc as catalysts.

Wallace et al. reported that an 18% yield of disulfide was obtained in 120 min during the oxidation of *n*-butyl mercaptan in the absence of catalyst, with 98% mercaptan conversion in about 21 h; however, in the absence of base, no oxidation occurred over 24 h [18]. Therefore, the presence of a base was essential. J. Zwart et al. [19,20] and A. Ryzhikov et al. [21] also pointed out that in the oxidation of mercaptans, the presence of additional base was necessary. Therefore, the base plays an important role in the catalysis of the oxidation of the mercaptans to disulfides.

For the base catalysts, the oxidation mechanism of *tert*-butyl thiol obeys base-catalyzed oxidation reaction mechanism, which conforms to the mechanism proposed by Wallace et al. [22]:



where B<sup>θ</sup> represents the base.

Search for new solid bases for the sweetening catalysts is still in progress. Magnesia is one of the strongest solid bases [23] and the coordination numbers of magnesium atom and oxygen atom are all 6. The low coordination of oxygen anion O<sup>2-</sup> is considered to

\* Corresponding author at: 4th Huayuan Road, Shilong industrial section, Men-tougou, Beijing, PR China. Tel.: +86 10 69809379; fax: +86 10 60800217.

E-mail address: [zyfbuct@sina.com](mailto:zyfbuct@sina.com) (Y. Zhang).

be responsible for its basicity. According to the proposal of Coluccia and Tench, several MgO ion pairs of other coordination numbers exist on the surface of this MgO, such as the corners, edges and high Miller index surfaces of the magnesia crystal, and the coordination numbers of the oxygen atom would be 3, 4 and 5 at these sites [24]. The crystal defects on the magnesia surface result in the imbalance of electronic charge of O<sup>2-</sup> anion, leading to the formation of strongly basic sites.

Gillespie et al. developed the solid solutions of metal oxides MgO/Al<sub>2</sub>O<sub>3</sub> and NiO/MgO/Al<sub>2</sub>O<sub>3</sub> for use as solid bases to catalyze the oxidation of mercaptans to disulfides successfully [25].

A novel catalyst which has adequate basicity and defects may solve the problems associated with desulfurization and octane value loss during the traditional gasoline hydro-desulfurization process. It is possible to completely eliminated aqueous sodium hydroxide by incorporating solid basic materials into the catalyst formation. Furthermore, the commonly used Merox process of sweetening is rather expensive since it involves expensive catalyst, such as CoPc, which is costly and cannot convert iso-mercaptans efficiently. Thus, a CoPc-free sweetening process could result in significant savings over the use of Merox process of sweetening.

The main objective of the present study was to find a lower-cost and more effective catalyst which has better stability capable of solving over proof mercaptans in hydrogenated gasoline, a series of solid-base catalysts with magnesia matrix were synthesized and tested in gas-liquid-solid heterogeneous base-catalyzed oxidation of mercaptans. Most of all, the critical factor that affects the conversion of *tert*-butyl thiol, such as basic centers and active oxygen species of solid-base catalysts were studied.

## 2. Experimental

### 2.1. Preparation of solid-base catalysts

The solid-base catalysts were prepared at ambient pressure and temperature. Light magnesia, NaOH, Cu(NO<sub>3</sub>)<sub>2</sub>·3H<sub>2</sub>O and Ni(NO<sub>3</sub>)<sub>2</sub>·6H<sub>2</sub>O purchased from Sinopharm Chemical Reagent Co. Ltd were of analytical grade. A series of solid-base catalysts used in this study were prepared via the protocol below: (1) preparation of sample A: the powders of 190 g light magnesia and 10 g palygorskite were mixed in a 500 mL beaker until the mixture was homogenous. 80 mL NaOH aq. solution was then added into the above mixture under constant stirring until the mixture was uniform. The concentration of NaOH solution of A is 3.3%. The mixture was then extruded and the extrudate was dried at 120 °C for 3 h and calcinated at 500 °C for 4 h. (2) Preparation of sample B and C: the powders of 190 g light magnesia and 10 g palygorskite were mixed in a 500 mL beaker until the mixture was homogenous. 80 mL aq. solution of NaOH and Cu(NO<sub>3</sub>)<sub>2</sub>·3H<sub>2</sub>O or Ni(NO<sub>3</sub>)<sub>2</sub>·6H<sub>2</sub>O was added into the above admixture under constant stirring until the mixture was uniform, and the concentration of solution of NaOH, Cu(NO<sub>3</sub>)<sub>2</sub>·3H<sub>2</sub>O and Ni(NO<sub>3</sub>)<sub>2</sub>·6H<sub>2</sub>O is 3.5%, 40.4% and 51.8%, respectively; then the mixture was extruded and the extrudate was dried at 120 °C for 3 h and calcinated at 500 °C for 4 h. (3) Preparation of sample D: the powders of 190 g light magnesia and 10 g palygorskite were mixed in a 500 mL beaker until the mixture was homogenous. 80 mL solution of NaOH, Cu(NO<sub>3</sub>)<sub>2</sub>·3H<sub>2</sub>O and Ni(NO<sub>3</sub>)<sub>2</sub>·6H<sub>2</sub>O was added into the above admixture under constant stirring until the mixture was uniform, and the concentration of solution of NaOH, Cu(NO<sub>3</sub>)<sub>2</sub>·3H<sub>2</sub>O and Ni(NO<sub>3</sub>)<sub>2</sub>·6H<sub>2</sub>O is 3.7%, 42.6% and 54.6%, respectively; then the mixture was extruded and the extrudate was dried at 120 °C for 3 h and calcinated at 500 °C for 4 h.

The composition and physical properties of samples are shown in Table 1.

### 2.2. Characterization methods

The hydroxyl groups of the catalysts were identified by FT-IR using a Nicolet 750 spectrometer (the resolution of spectrometer is 0.125 cm<sup>-1</sup>) in the range of 4000–3000 cm<sup>-1</sup> at a resolution of 4.0 cm<sup>-1</sup> using the KBr pellet technique. The structure of CO<sub>2</sub> chemisorbed on samples was also determined by FT-IR, the method of catalysts pretreatment corresponded to previous literatures [26,27].

X-ray diffraction (XRD) technique was used to characterize the crystal structure. A D8 ADVANCE X-ray diffractometer equipped with Ni-filtrated Cu-K $\alpha$  radiation source (40 kV, 40 mA) was used. Samples were analyzed with the continuous scan mode at 2°/min over a 2 $\theta$  range of 5–80°.

Temperature programmed desorption (TPD) of oxygen, CO<sub>2</sub> and H<sub>2</sub> was carried out on a FINESORB-3010 apparatus; the samples were treated at 400 °C for an hour in oxygen (or CO<sub>2</sub> or H<sub>2</sub>) and cooled to room temperature in the same atmosphere then swept with helium at a rate of 30 mL/min until the chromatogram has steadied. Finally, the sample was heated at a rate of 20 °C/min in helium for recording the TPD spectra.

The electron paramagnetic resonance (EPR) spectra were obtained at room temperature by a JEOL JES FA200 machine. The concentration of 5,5-dimethyl-1-pyrroline N-oxide (DMPO) radical trap was 1 mol/L.

### 2.3. Catalytic test for oxidation of *tert*-butyl thiol

*Tert*-butyl thiol was considered as the model compound representative of iso-mercaptans in hydrogenated gasoline [28]. It was dissolved in *n*-hexane, air was used as the oxidizing agent.

The catalytic performance of the solid-base samples were compared to a commercial CoPc catalyst. A conventional fixed bed flow reactor (1.2 in. i.d.) was used for the catalysts performance tests. 6 mL of catalyst was crushed to particles of 40–60 mesh and packed in the reactor. Liquid stream and the catalyst were in neat contact with each other as the liquid stream flowed upwardly through the catalyst. Contact time was equivalent to a liquid hourly space velocity (LHSV) of 3.0 h<sup>-1</sup> or 1.0 h<sup>-1</sup>. Air, at flows of 6 mL/min, passed through the reactor at 40 °C. The apparatus was consisted of thermostat water bath maintained by recycling water with a pump. A static mixer was placed in front of the reactor to extensively mix acid hydrocarbon with air.

The feedstock was *tert*-butyl thiol dissolved in *n*-hexane with the initial mercaptan-type sulfur content of 75 weight ppm; when the treating time reached 6 h, the mercaptan-type sulfur content was 1513 mass ppm. When the conversion rate of *tert*-butyl thiol decreased to a level of 80% or below, the catalysts were thought to be inactive and the evaluation tests were ceased.

The contents of mercaptan-type sulfur were measured by potentiometric titration according to ASTM D3227-83. Products were identified with GC-MS.

## 3. Results

### 3.1. Measurement of sweetening reactivity

In order to clarify the property of the catalyst specific to catalyze the oxidation of *tert*-butyl thiol, the catalytic performances of synthesized solid-base catalysts were compared with that of a commercial CoPc catalyst. The conversions are shown in Fig. 1. According to the analysis result of GC-MS, the oxidation product of the *tert*-butyl thiol is disulfide whose figure of mass spectrum is as shown in Fig. 2, which is consistent with the base-catalyzed oxidation reaction mechanism of *tert*-butyl thiol mentioned above.

**Table 1**  
Characterization of solid-base catalysts.

Catalyst ID	Type	NaOH (wt.%)	BET surface area ( $\text{m}^2/\text{g}$ )	Pore volume ( $\text{cm}^3/\text{g}$ )	Pore diameter at the maximum (nm)
A	NaOH/MgO	1.3	39.8	0.30	23.2
B	CuO/NaOH/MgO	1.3	17.8	0.09	30.9
C	NiO/NaOH/MgO	1.3	24.8	0.14	33.5
D	CuO/NiO/NaOH/MgO	1.3	20.1	0.12	34.0

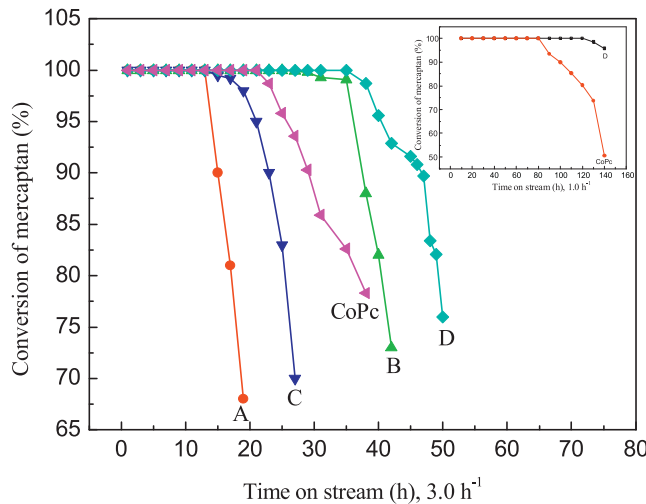


**Fig. 1.** *tert*-Butyl thiol oxidation activity over developed and commercial catalysts.

**Fig. 1** shows that the initial conversion of *tert*-butyl thiol at  $3.0\text{ h}^{-1}$  of LHSV was 100% of all catalysts; the sweetening performance of the solid-base catalysts is in the order: D>B>CoPc>C>A. The results show that the stability of sample D is 10 h longer than the commercial catalyst CoPc at  $3.0\text{ h}^{-1}$  of LHSV. **Fig. 1** also shows the conversion of *tert*-butyl thiol at  $1.0\text{ h}^{-1}$  of LHSV and the results demonstrate that under lower LHSV, i.e., longer contact time of catalysts and *tert*-butyl, the lifetime of catalysts increased sharply. And moreover, the sweetening performance of the solid-base catalyst D was much better than that of CoPc catalyst. When ran to 140 h, the conversion of *tert*-butyl thiol on CoPc catalyst reduced to 50.6% whereas the conversion of *tert*-butyl thiol on the solid-base catalyst

D was 95.7%. Obviously, the sweetening performance of the modified MgO is much better than that of the commercial CoPc catalyst.

### 3.2. Basicity analysis of solid-base catalysts

As mentioned above, the first step of mercaptan oxidation is the formation of mercaptide ion, so the basicity of the catalyst has a significant impact on the catalytic performance in mercaptan oxidation reactions.

#### 3.2.1. FT-IR

The hydroxyl groups on the surface of the solid also act as basic sites and have been shown to promote basic reaction. OH groups of MgO are also involved in basic reactivity, with an even higher catalytic reactivity than that of oxide ions [29–32]. It has been reported that different types of OH groups are present on the surface of magnesium oxide, which do not disappear completely at calcination temperatures below  $900^\circ\text{C}$  [33,34]. **Fig. 3** shows the FT-IR spectrums of the samples in the range of  $4000\text{--}3000\text{ cm}^{-1}$ . The most of hydroxyl groups on catalysts are OH groups associated through H-bonding, represented by a broad peak in range of  $3000\text{--}3600\text{ cm}^{-1}$ . And some isolated OH groups were also observed on samples, as indicated by a narrow band around  $3700\text{ cm}^{-1}$ .

The chemical state of surface oxygen bonded to adsorbed  $\text{CO}_2$  species gives an indication of basic site structure and strength. Three species of carbonates could be formed, the unidentate carbonate, the bidentate carbonate and the bicarbonate [35].

The FT-IR spectrums of the pre-adsorbed  $\text{CO}_2$  on samples A to D are shown in **Fig. 4**. It can be seen that there are only medium basic sites (asymmetric O—C—O stretching at  $1630\text{ cm}^{-1}$ ) on sample A. Furthermore, when CuO and NiO were doped, some of medium basic sites became strong basic centers (symmetric O—C—O stretching at around  $1384\text{ cm}^{-1}$ ).

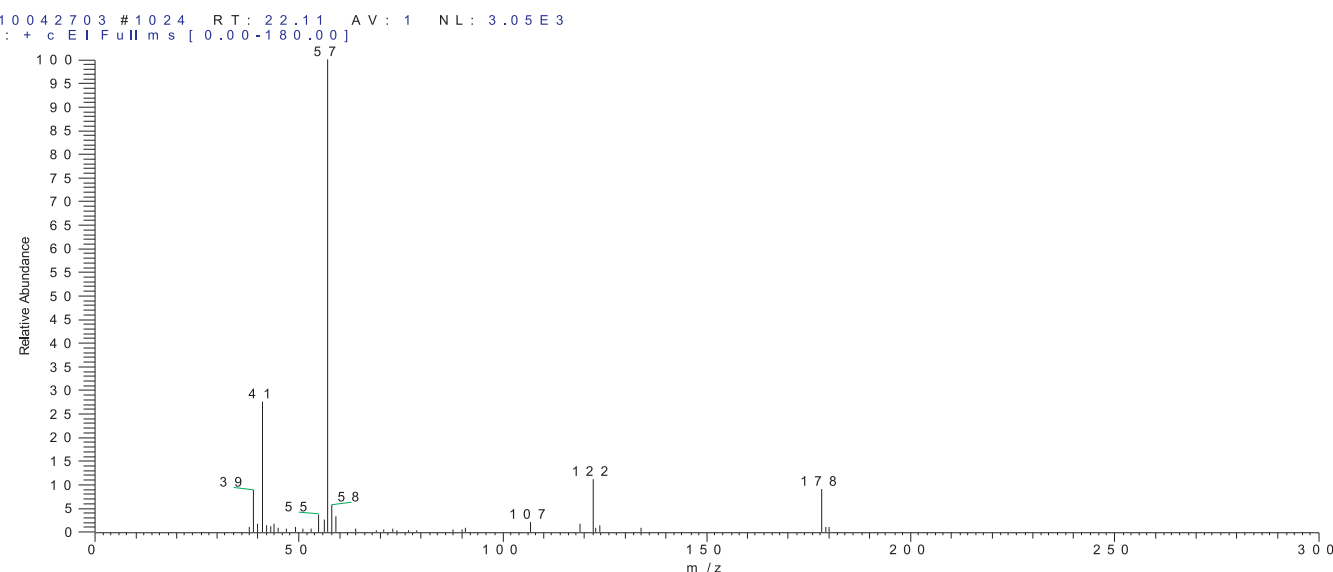


**Fig. 2.** Mass spectrum of disulfide of di-*tert*-butyl.

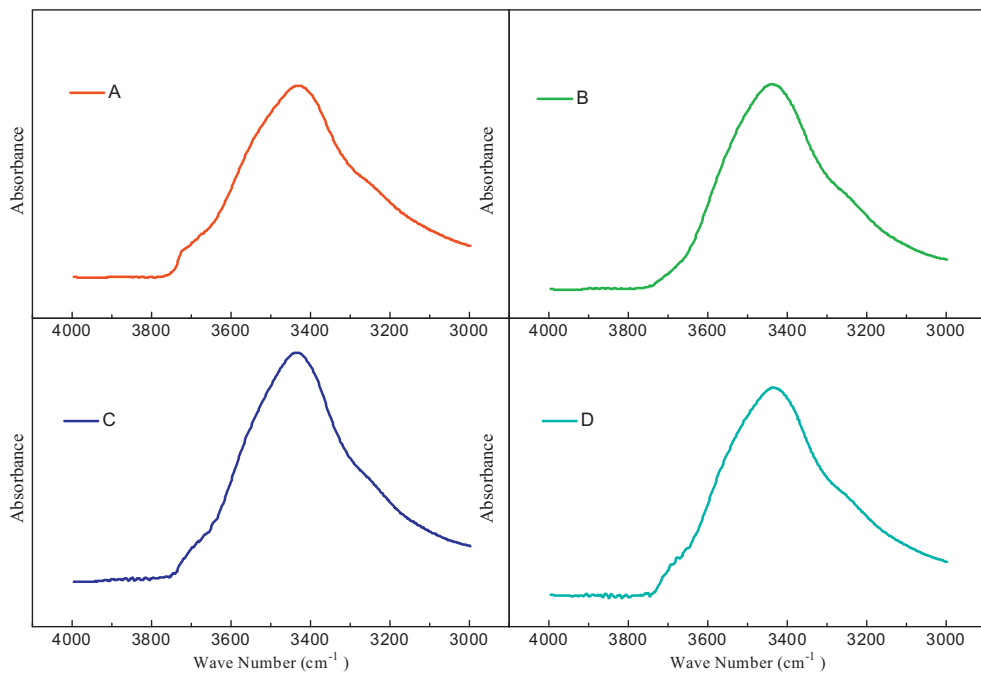
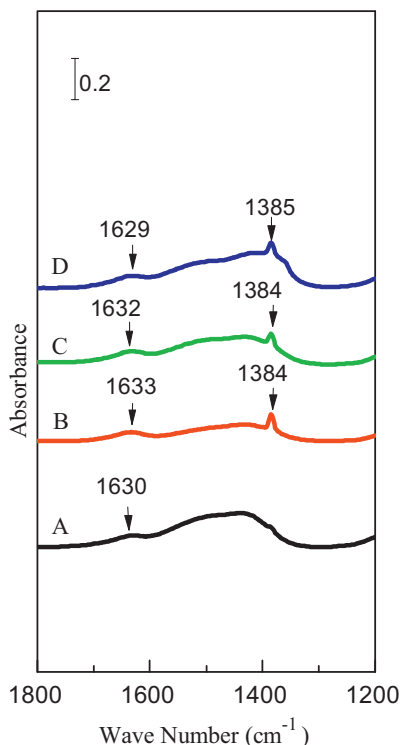


Fig. 3. FT-IR spectra of the solid-base catalysts.

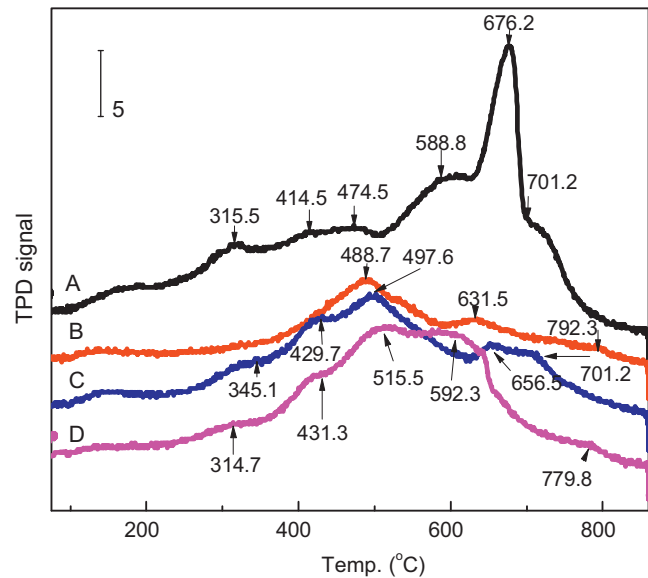
### 3.2.2. CO<sub>2</sub>-TPD

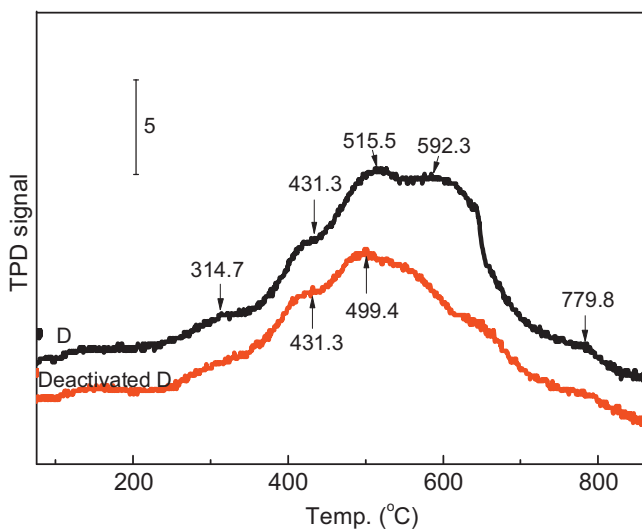
Fig. 5 depicts the TPD profiles of CO<sub>2</sub> adsorbed on solid-base catalysts. Fig. 5 shows that there are different types of basic centers on solid-base catalysts. Combine the results of FT-IR, the CO<sub>2</sub> desorption peaks ( $T_{CO_2}$ ) below 400 °C can be assigned to weak basic centers, the CO<sub>2</sub> desorption peaks between 400 °C and 700 °C can be assigned to medium basic centers and the CO<sub>2</sub> desorption peaks above 700 °C represents strong basic centers.

Fig. 4. FT-IR spectra of pre-adsorbed CO<sub>2</sub> on the solid-base catalysts.

It can be seen from Fig. 5 that doping of CuO and NiO to the catalyst contributes to the formation of basic centers. Metal ions with ionic radii similar to that of Mg<sup>2+</sup> can easily replace Mg<sup>2+</sup> in the MgO crystalline lattice. The replacement results in a deformed crystalline lattice and imbalanced electron charge distribution, thereby increasing the basicity. Among transition metal ions, copper ion is the most effective while nickel ion ranks second [36]. Furthermore, the interaction between copper ions and nickel ions can produce more defects, which result in lower coordination number of O<sup>2-</sup> and more unsaturated oxygen atoms.

According to the aforementioned experimental observations, it became evident that the oxidation of *tert*-butyl thiol is closely related to the base strength and the basic sites with stronger strength appeared to be the active sites for the oxidation of *tert*-butyl thiol.

Fig. 5. CO<sub>2</sub>-TPD profiles of the solid-base catalysts.



**Fig. 6.**  $\text{CO}_2$ -TPD profiles of fresh sample D and deactivated D.

The  $\text{CO}_2$ -TPD plots of fresh sample D and deactivated D are shown in Fig. 6. As it is shown in Fig. 6, it can be seen that weak basic center  $T_{\text{CO}_2} = 314.7^\circ\text{C}$ , medium basic center  $T_{\text{CO}_2} = 592.3^\circ\text{C}$  and strong basic center  $T_{\text{CO}_2} = 779.8^\circ\text{C}$  all disappeared after deactivation. This clearly suggested that all of the three different types of basic centers participated in the reaction. Furthermore, the strength of medium basic center  $\text{CO}_2$  desorption peak at  $515.5^\circ\text{C}$  weakened to  $499.4^\circ\text{C}$  after deactivation. These observations lead us to conclude that the basic sites responsible for the sweetening reactivity of the catalysts being studied are mainly the medium and strong basic centers. The more amount and the stronger strength of basic centers, the higher catalytic reactivity of catalysts.

### 3.2.3. $\text{H}_2$ -TPD

Hydrogen adsorption on active sites of  $\text{MgO}$  surfaces was used to estimate intrinsic surface states of coordinatively unsaturated ions at imperfect surface sites. And the active sites for hydrogen adsorption have a common basic structure of  $\text{O}_{\text{LC}}^{2-} - \text{Mg}_{\text{LC}}^{2+}$  (a subscript denotes a low coordination state). A pair of  $\text{O}_{\text{LC}}^{2-}$  and  $\text{Mg}_{\text{LC}}^{2+}$  in highly coordinative unsaturation forms the active site. Approaching this pair site,  $\text{H}_2$  is forced to polarize into  $\text{H}^+ - \text{H}^-$  by the cooperative actions of the electron-donor (or Lewis basicity) and electron-acceptor (or Lewis acidity) activities of  $\text{O}_{\text{LC}}^{2-}$  and  $\text{Mg}_{\text{LC}}^{2+}$ , respectively, and finally heterolytic dissociation takes place. A proton adsorbed on  $\text{O}_{\text{LC}}^{2-}$  becomes  $\text{OH}^-$  and a  $\text{H}^-$  ion is stabilized on  $\text{Mg}_{\text{LC}}^{2+}$ . Besides, it predicts a remarkable increase in the electron-donor (namely, basic) property of  $\text{O}_{\text{LC}}^{2-}$  with a decrease in the coordination number, while the electron-acceptor (namely, acidic) property of  $\text{Mg}_{\text{LC}}^{2+}$  is remarkably lowered with a decrease in the coordination number [37–39].

$W_2$  and  $W_3$  species on the  $\text{H}_2$ -TPD spectra of the solid-base catalysts, as shown in Table 2, were determined to be  $\text{O}_{4\text{C}}^{2-} - \text{Mg}_{3\text{C}}^{2+}$ ,  $W_4$

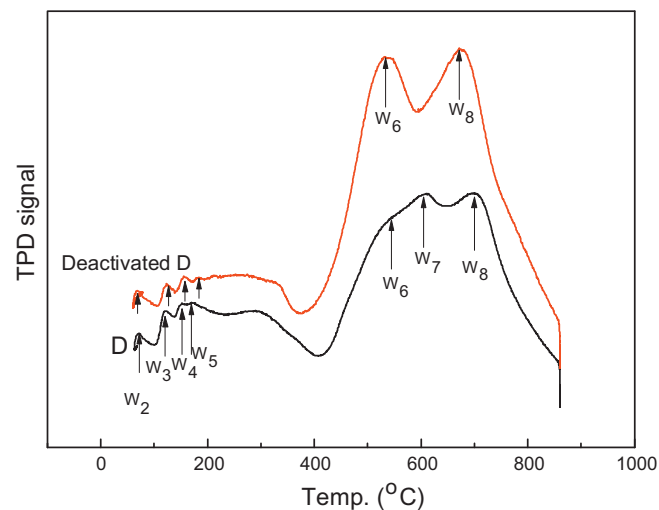


**Fig. 7.**  $\text{H}_2$ -TPD profiles of fresh sample D and deactivated D.

and  $W_5$  species were determined to be  $\text{O}_{3\text{C}}^{2-} - \text{Mg}_{4\text{C}}^{2+}$ , and  $W_6$ – $W_8$  species were determined to be  $\text{O}_{3\text{C}}^{2-} - \text{Mg}_{3\text{C}}^{2+}$  in various coordinative environments (a subscript denotes a coordination number) [37].

Because it predicts a remarkable increase in the electron-donor (namely, basic) property of  $\text{O}_{\text{LC}}^{2-}$  with a decrease in the coordination number, while the electron-acceptor (namely, acidic) property of  $\text{Mg}_{\text{LC}}^{2+}$  is remarkably lowered with a decrease in the coordination number [38,39]. Therefore, the  $W_8$  species is the strongest basic center.

The  $\text{H}_2$ -TPD plots of fresh sample D and deactivated D are shown in Fig. 7. As shown in Fig. 7, it can be seen that there is no obvious change in the spectra of  $W_2$ – $W_5$  species on fresh sample D and deactivated D. However, the temperature of desorption peak of  $W_6$  decreased after deactivation (from  $547.6^\circ\text{C}$  to  $538.7^\circ\text{C}$ ), the desorption peak of  $W_7$  disappeared after deactivation, which is in consistent with the  $\text{CO}_2$ -TPD results that one of the medium basic centers disappeared and the basic strength of the other weakened after deactivation. Furthermore, the temperature of desorption peak of  $W_8$  also decreased after deactivation (from  $699.4^\circ\text{C}$  to  $676.2^\circ\text{C}$ ), which is also in consistent with the  $\text{CO}_2$ -TPD results that strong basic center disappeared after deactivation. These facts support the view that the active sites of  $W_2$ – $W_5$  for hydrogen adsorption are weak basic centers,  $W_6$  and  $W_7$  are medium basic centers, and  $W_8$  are strong basic centers. It is, therefore, reasonable to expect that the pairs of  $\text{O}_{4\text{C}}^{2-} - \text{Mg}_{3\text{C}}^{2+}$  and  $\text{O}_{3\text{C}}^{2-} - \text{Mg}_{4\text{C}}^{2+}$  afford weak basic centers, part of  $\text{O}_{3\text{C}}^{2-} - \text{Mg}_{3\text{C}}^{2+}$  provide medium basic centers while the other part of  $\text{O}_{3\text{C}}^{2-} - \text{Mg}_{3\text{C}}^{2+}$  supply strong basic centers based on the difference in coordination numbers of  $\text{O}_{\text{LC}}^{2-}$  and  $\text{Mg}_{\text{LC}}^{2+}$  and the difference in coordination number of the next nearest ions around  $\text{O}_{\text{LC}}^{2-}$  and  $\text{Mg}_{\text{LC}}^{2+}$  [37].

### 3.3. Crystalline phase

As shown in Fig. 8, XRD patterns of all samples revealed the main characteristic peaks of magnesia, and peaks of  $\text{NiO}$  or  $\text{CuO}$  are not observed. This proved that the  $\text{NiO}$  and  $\text{CuO}$  phase were spread on the surface of the  $\text{MgO}$  support in amorphous form or a solid solution is formed.

### 3.4. Studies on the active oxygen species

#### 3.4.1. EPR

The solid-base catalysts were dispersed in dimethyl sulfoxide to simulate the environment of sweetening, with DMPO as radical

**Table 2**  
Analysis-results of  $\text{H}_2$ -TPD of the solid-base catalysts.

	Desorption temperature ( $^\circ\text{C}$ )						
	$W_2$	$W_3$	$W_4$	$W_5$	$W_6$	$W_7$	$W_8$
A	70.8	122.6	172.6	254.8	606.5	653.0	679.8
B	70.8	120.8	149.4	172.6	554.8	672.6	738.7
C	70.8	128.0	160.1	183.3	570.8	–	695.8
D	70.8	122.6	154.8	172.6	547.6	611.9	699.4

The superoxide anions and basic sites result from surface defects play an important role in conversion of iso-mercaptans.

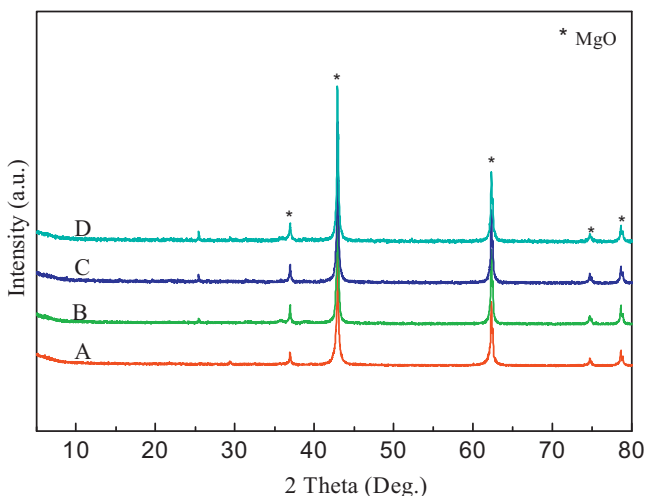


**Fig. 8.** XRD patterns of the solid-base catalysts.

trap. The EPR spectra of radical trap of the catalysts are given in Fig. 9. The signal of  $g=2.0023$ ,  $aN=1.461$  mT,  $aH^\alpha=1.404$  mT and  $aH^\beta=0.094$  mT can be assigned to superoxide anions,  $O_2^-$ . It is clearly shown that the amount of superoxide anions of different samples is different from each other, and the amount of superoxide anions on catalysts is in the sequence: D>B>C>A, which is in accordance with the sequence of the reactivity of the catalysts. It explicitly indicates that the active oxygen species in favour of catalysis oxidation of *tert*-butyl thiol are superoxide anions. The more amount of superoxide anions on the surface of catalysts, the better reactivity of the catalysts.

#### 3.4.2. $O_2$ -TPD

Catalytic oxidation is one of the most interesting reactions in heterogeneous catalysis. For an understanding of it, it would be very important to know the adsorption state of oxygen [40].

Fig. 10 shows the TPD profiles of oxygen for the solid-base catalysts. There exists three desorption peaks of oxygen ( $T_{O_2}$ , denoted by  $\alpha$ ,  $\beta$  and  $\gamma$  respectively) on samples. According to the literature [41] and on the basis of the results of FT-IR, the  $\alpha$  peak in a temperature range of  $100^\circ\text{C} < T_{O_2} < 400^\circ\text{C}$  could be assigned to the hydroxyl oxygen ( $O^-$ ).

Combined with the results of FT-IR and ESR, the  $\beta$  oxygen desorption peaks on sample B, C and D in the temperature range of

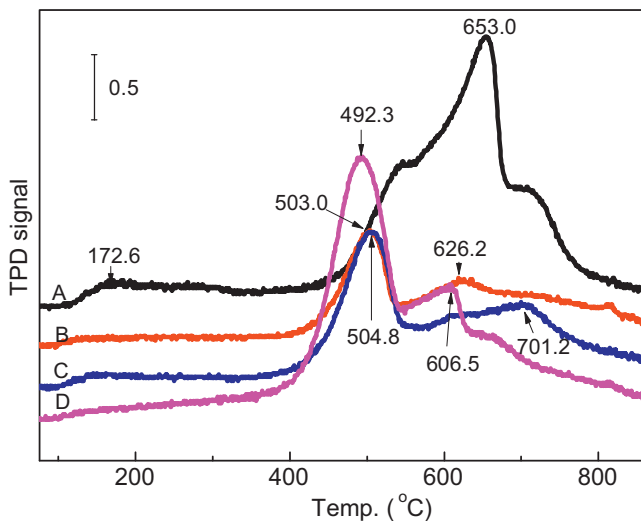


**Fig. 10.** TPD profiles of oxygen for the solid-base catalysts.

$490^\circ\text{C} < T_{O_2} < 520^\circ\text{C}$  could be assigned to the adsorbed oxygen ( $O_2^-$ ). Moreover, the order of the mobility of adsorbed oxygen in different solid-bases could be given below: D( $T_{O_2}=492.3^\circ\text{C}$ )>B( $T_{O_2}=503.0^\circ\text{C}$ )>C( $T_{O_2}=504.8^\circ\text{C}$ ), and there is no obvious  $\beta$  oxygen desorption peak on sample A, which is in agreement with the sequence of sweetening reactivity of catalysts. This confirmed once more that the active oxygen species for catalysis oxidation of *tert*-butyl thiol are superoxide anions,  $O_2^-$ .

Besides, there are also desorption peaks of lattice oxygen  $O^{2-}$  (denoted by  $\gamma$ ) located between the temperature range of  $605^\circ\text{C}-705^\circ\text{C}$  on samples, and the sequence of the mobility of  $\gamma$  oxygen on different solid-bases is as follows: D( $T_{O_2}=606.5^\circ\text{C}$ )>B( $T_{O_2}=626.2^\circ\text{C}$ )>A( $T_{O_2}=653.0^\circ\text{C}$ )>C( $T_{O_2}=701.2^\circ\text{C}$ ). The weaker the adsorption of  $\gamma$  oxygen on the catalyst is, the larger the mobility of lattice oxygen is. The smaller mobility of lattice oxygen in sample C may be ascribed to the formation of NiO-MgO solid solutions.

The  $O_2$ -TPD plots of fresh sample D and deactivated D are shown in Fig. 11. As shown in Fig. 11, it can be seen that the quantity of  $\beta$  oxygen decreased significantly after deactivation, and its mobility was also weakened significantly (from  $T_{O_2}=492.3^\circ\text{C}$  to  $511.9^\circ\text{C}$ ). This again confirms that the active oxygen species for catalysis

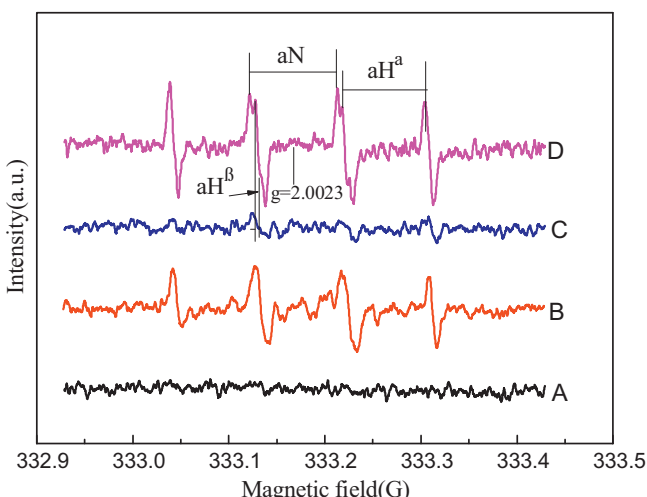


**Fig. 9.** EPR spectra of radical trap of the solid-base catalysts.

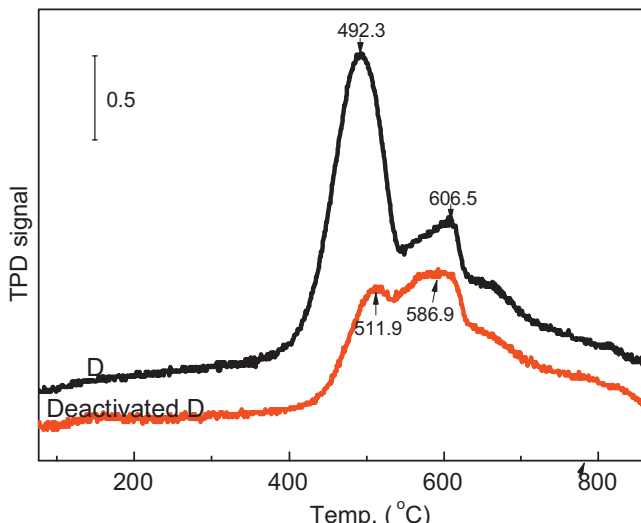


**Fig. 11.** TPD profiles of oxygen for fresh sample D and deactivated D.

oxidation of tert-butyl thiol are superoxide anions, the larger the mobility and the more amount of  $\beta$  oxygen, the higher catalytic reactivity of catalysts.

#### 4. Discussion

The synthesized solid-base catalysts displayed better stabilities compared with the commercial sweetening catalyst CoPc. The incorporation of transition metal ions with MgO results in a deformed crystalline lattice and an imbalanced electron charge distribution. This creates a large number of electron rich centers and other electron-trapping structural defects on the surface of the MgO. When these traps are close enough to the surface, the trapped electrons can react with electron acceptor oxygen O<sub>2</sub> forms adsorbed superoxide anions [42]. In addition, the electron removal is assisted by metal atoms or clusters deposited on the surface of the particles.

Based on the above argument, it became evident that the active sites responsible for the sweetening reactivity of the catalysts being studied are defects and basic centers. The active oxygen species for catalysis oxidation of iso-mercaptans are superoxide anions. The doping of Cu<sup>2+</sup> and Ni<sup>2+</sup> not only enhances basicity, but also increases electron deficiency, improves the efficiency of electron transfer, leading to higher reactivity of catalyst because of steric hindrance of iso-mercaptans.

Based on our best knowledge, the present study is the first to report that the active oxygen species for catalysis oxidation of iso-mercaptans are superoxide anions, O<sub>2</sub><sup>-</sup>, the larger the mobility and the more amount of O<sub>2</sub><sup>-</sup>, the higher catalytic reactivity of catalysts. In addition, the basic sites responsible for the reactivity are mainly the medium and strong basic centers. The more amount and the stronger strength of basic centers, the higher catalytic reactivity of catalysts. Furthermore, the active sites of O<sub>4C</sub><sup>2-</sup>–Mg<sub>3C</sub><sup>2+</sup> and O<sub>3C</sub><sup>2-</sup>–Mg<sub>4C</sub><sup>2+</sup> afford weak basic centers, part of O<sub>3C</sub><sup>2-</sup>–Mg<sub>3C</sub><sup>2+</sup> provide medium basic centers while the other part of O<sub>3C</sub><sup>2-</sup>–Mg<sub>3C</sub><sup>2+</sup> supply strong basic centers based on the difference in coordination numbers of O<sub>LC</sub><sup>2-</sup> and Mg<sub>LC</sub><sup>2+</sup> and the difference in coordination number of the next nearest ions around O<sub>LC</sub><sup>2-</sup> and Mg<sub>LC</sub><sup>2+</sup>.

#### 5. Conclusion

A novel sweetening catalyst was explored for gas–liquid–solid heterogeneous base-catalyzed oxidation of iso-mercaptans in hydrogenated gasoline. Compared with the commercial catalyst CoPc, the catalyst explored in this paper showed better stability.

The present study found that the active oxygen species for catalysis oxidation of iso-mercaptans are superoxide anions, O<sub>2</sub><sup>-</sup>. Moreover, it is found that the basic sites responsible for the reactivity are mainly the medium and strong basic centers. As a result, it is found that in the gas–liquid–solid heterogeneous oxidation reaction, the reactivity of a catalyst is not only correlated to basicity, but also to the electronic effect and steric effect. The active sites of O<sub>4C</sub><sup>2-</sup>–Mg<sub>3C</sub><sup>2+</sup> and O<sub>3C</sub><sup>2-</sup>–Mg<sub>4C</sub><sup>2+</sup> afford weak basic centers, part of O<sub>3C</sub><sup>2-</sup>–Mg<sub>3C</sub><sup>2+</sup> provide medium basic centers while the other part of O<sub>3C</sub><sup>2-</sup>–Mg<sub>3C</sub><sup>2+</sup> supply strong basic centers based on the difference in coordination numbers of O<sub>LC</sub><sup>2-</sup> and Mg<sub>LC</sub><sup>2+</sup> and the difference in coordination number of the next nearest ions around O<sub>LC</sub><sup>2-</sup> and Mg<sub>LC</sub><sup>2+</sup>.

O<sub>3C</sub><sup>2-</sup>–Mg<sub>3C</sub><sup>2+</sup> supply strong basic centers based on the difference in coordination numbers of O<sub>LC</sub><sup>2-</sup> and Mg<sub>LC</sub><sup>2+</sup> and the difference in coordination number of the next nearest ions around O<sub>LC</sub><sup>2-</sup> and Mg<sub>LC</sub><sup>2+</sup>.

#### References

- [1] S. Hatanaka, M. Yamada, Ind. Eng. Chem. Res. 36 (1997) 5110–5117.
- [2] C. Song, X. Ma, Appl. Catal. B 41 (2003) 207–238.
- [3] T.G. Kaufmann, A. Kaldor, G.F. Stuntz, M.C. Kerby, L.L. Ansell, Catal. Today 62 (2000) 77–90.
- [4] I.V. Babich, J.A. Moulijn, Fuel 82 (2003) 607–631.
- [5] J.T. Miller, W.J. Reagan, J.A. Kaduk, C.I. Marshall, A.J. Kropf, J. Catal. 193 (2000) 123–131.
- [6] P.H. Desai, S.L. Lee, R.J. Jonker, M. De Boer, J. Vrieling, M.S. Sarli, Fuel Reformul. (November/December) (1994) 43–52.
- [7] S. Hatanaka, M. Yamada, Ind. Eng. Chem. Res. 36 (1997) 1519–1523.
- [8] S. Hatanaka, M. Yamada, Ind. Eng. Chem. Res. 37 (1998) 1748–1754.
- [9] N.D. Santos, H. Dulot, N. Marchal, M. Vrinat, Appl. Catal. A 352 (2009) 114–123.
- [10] S. Brunet, D. Mey, G. Péröt, C. Bouchy, F. Diehl, Appl. Catal. A 278 (2005) 143–172.
- [11] D.E. Jiang, B.Y. Zhao, H.Z.H. Huang, Y.C.H. Xie, G.C.H. Pan, G.P. Ran, E.Z. Min, Appl. Catal. A 192 (2000) 1–8.
- [12] D.E. Jiang, B.Y. Zhao, Y.C. Xie, G.C. Pan, G.P. Ran, E.Z. Min, Appl. Catal. A 219 (2001) 69–78.
- [13] I. Chatti, A. Ghobel, P. Grange, J.M. Colin, Catal. Today 75 (2002) 113–117.
- [14] J.J. Alcaraz, B.J. Arena, R.D. Gillespie, J.S. Holmgren, Catal. Today 43 (1998) 89–99.
- [15] D.E.G. Jiang, B. Pan, Zhao, G. Ran, Y. Xie, E.Z. Min, Appl. Catal. A 201 (2000) 169–176.
- [16] H. Mei, M. Hu, H.X. Ma, H.Q. Yao, J. Shen, Fuel Process. Technol. 88 (2007) 343–348.
- [17] V.I. Iliev, A.I. Ileva, L.D. Dimitrov, Appl. Catal. A 126 (1995) 333–340.
- [18] T.J. Wallace, A. Schriesheim, H. Hurwitz, M.B. Glaser, Ind. Eng. Chem. Process Des. Dev. 3 (1964) 237–241.
- [19] J. Zwart, H.C.V.D. Weide, N. Bröker, C. Rummens, G.C.A. Schuit, J. Mol. Catal. 3 (1977/78) 151–163.
- [20] T.A.M.M. Maas, M. Kuijer, J. Zwart, J. Chem. Soc. Chem. Commun. (1976) 86–88.
- [21] A. Ryzhikov, V. Hulea, D. Tichit, C. Leroi, D. Anglerot, B. Coq, P. Trens, Appl. Catal. A 397 (2011) 218–224.
- [22] T.J. Wallace, A. Schriesheim, W. Bartok, J. Org. Chem. 28 (1963) 1311–1314.
- [23] J.I. Take, N. Kikuchi, Y. Yoneda, J. Catal. 21 (1971) 164–170.
- [24] S. Coluccia, A.J. Tench, Proceedings of the 7th International Congress on Catalysis, Tokyo, 1980, p. 1160.
- [25] R.D. Gillespie, J.S. Holmgren, U.S. Patent No. 3,40,465 (1994).
- [26] J.I.D. Cosimo, V.K. Díez, M. Xu, E. Iglesia, C.R. Apesteguía, J. Catal. 178 (1998) 499–510.
- [27] V.K. Díez, C.A. Ferretti, P.A. Torresi, C.R. Apesteguía, J.I.D. Cosimo, Catal. Today 173 (2011) 21–27.
- [28] L.J. Zhu, D.H. Xia, Y.Z. Xiang, Chem. Eng. Oil Gas (China) 38 (2009) 494–497.
- [29] G. Zhang, H. Hattori, K. Tanabe, Appl. Catal. 36 (1988) 189–197.
- [30] M.F. Hoq, I. Nieves, K.J. Klubunde, J. Catal. 123 (1990) 349–363.
- [31] C. Chizallet, G. Costentin, H.L. Pernot, J.M. Krafft, P. Bazin, J. Saussey, F. Delbecq, P. Sautet, M. Che, Oil Gas Sci. Technol. 61 (2006) 479–488.
- [32] M.L. Baily, C. Chizallet, G. Costentin, J.M. Krafft, H.L. Pernot, M. Che, J. Catal. 235 (2005) 413–422.
- [33] J. Puriwat, W. Chaitree, K. Suriye, S. Dokjampa, P. Praserthdam, J. Panpranot, Catal. Commun. 12 (2010) 80–85.
- [34] J.X. Li, W.L. Dai, K.N. Fan, J. Phys. Chem. C 112 (2008) 17657–17663.
- [35] J.I.D. Cosimo, V.K. Díez, C.R. Apesteguía, Appl. Clay Sci. 13 (1998) 433–449.
- [36] K. Tanabe, M. Misono, Y. Ono, H. Hattori, New Solid Acids and Bases: Their Catalytic properties, Kodansha LTD./ELSEVIER science publishers B.V., Tokyo/Amsterdam, 1989, pp. 114.
- [37] T. Ito, M. Kuramoto, M. Yoshioka, T. Tokuda, J. Phys. Chem. 87 (1983) 4411–4416.
- [38] T. Ito, T. Sekino, N. Moriai, T. Tokuda, J. Chem. Soc. Faraday Trans. 77 (1) (1981) 2181–2192.
- [39] T. Ito, T. Murakami, T. Tokuda, J. Chem. Soc. Faraday Trans. 79 (1) (1983) 913–924.
- [40] M. Iwamoto, Y. Yoda, M. Egashira, T. Seiyama, J. Phys. Chem. 80 (16) (1976) 1989–1994.
- [41] Z. Zhao, X.G. Yang, Y. Wu, Catal. Appl. B 8 (1996) 281–297.
- [42] G. Heinz, H. Adarn, J. Phys. Chem. 95 (1991) 5261–5267.